Physica A 515 (2019) 519–525

Contents lists available at ScienceDirect

Physica A

journal homepage: www.elsevier.com/locate/physa

Parametric perturbation in a model that describes the neuronal membrane potential

Diogo Ricardo da Costa [a,*], Matheus Hansen [b], Antonio Marcos Batista [c,d]

[a] Departamento de Física - UNESP, 13506-900, Rio Claro, SP, Brazil
[b] Instituto de Física - Universidade de São Paulo, 05314-970, São Paulo, SP, Brazil
[c] Departamento de Matemática e Estatística - UEPG, 84030-000, Ponta Grossa, PR, Brazil
[d] Potsdam Institute for Climate Impact Research, 14473, Potsdam, Germany

HIGHLIGHTS

- Parametric perturbation in the Rulkov mapping.
- A model that describes the neuronal membrane potential is studied.
- The system presents periodic behavior followed by chaotic bursts.
- We show how is the organization of the periodic regions in the parameter space.

ARTICLE INFO

Article history:
Received 5 March 2018
Received in revised form 10 July 2018
Available online 27 September 2018

Keywords:
Rulkov map
Shrimps
Parametric perturbation

ABSTRACT

The Rulkov mapping is a phenomenological model that simulates the changes in the neuronal membrane potential. In this work, we introduce a parametric perturbation in the Rulkov map, that can be related to an unexpected behavior, such as a malfunction of the neuronal membrane due to pathologies. The perturbed system still keeps its main characteristics, which includes periodic behavior followed by chaotic bursts. We verify the existence of a set of periodic regions, known as shrimps, embedded in chaotic attractors in the system with parametric perturbation. Some changes in the phase space, time evolution of the variables and bifurcation diagrams are observed. Finally, we show the extreming curves, which demonstrate how is the organization of the periodic regions in the parameter space.

1. Introduction

With the develop of fast computers, the study of dynamical systems has attracted a lot of attention during the last years. In particular, dissipative dynamical systems have helped the researchers to describe several phenomena from diverse areas of science, such as physics [1,2], economics [3], biology [4,5], and mathematics [6,7]. In general, dynamical systems have been mathematically modeled by means of nonlinear equations [8] or N-dimensional nonlinear mappings [9,10]. One of the most important aspects of dynamical system is to understand its properties in the phase space. In the case of dissipative systems, information about the periodicity of orbits and bifurcations are fundamental to make predictions about the asymptotic behavior of the dynamics.

The study of attractors and its evolution has attracted much attention from the scientific community. In this sense, we propose to study the two dimensional mapping formulated by Rulkov [11] to describe the neuronal membrane potential.

* Corresponding author.
E-mail address: diogo_cost@hotmail.com (D.R. da Costa).

https://doi.org/10.1016/j.physa.2018.09.160
0378-4371/

The Rulkov map is from the computational point of view very simple to iterate than other models, beside that, its dynamics exhibits interesting properties in the phase space, such as bifurcations and attractors. It has been applied in the description of neuronal networks [12].

Our goal is to study the origin and the evolution of attractors in the Rulkov map, where we introduce a parametric perturbation. In literature, there are experimental and theoretical results about the effects of parametric perturbation in dynamics systems. Fronzoni et al. [13] reported experimental evidence of chaos suppression by parametric perturbations in magnestoelastic beam systems. Parametric perturbation can be used to control chaotic behavior [14,15] and to synchronize coupled systems [16]. Deivasundari et al. [17] observed the existence of transition from ordered to chaotic behavior in voltage-mode controlled buck converter under parametric perturbation. In this work, we consider the perturbation in the nonlinearity parameter of the Rulkov map. This parameter controls the variable that is related to the membrane potential of the neuron. Depending on the parameter value, the neuron can display chaotic bursts or continuous chaotic oscillations [18]. This way, the parametric perturbation can change the chaotic behavior. Alteration in membrane potential can be associated with pathologies [19].

We show periodic self similar structures embedded in chaotic regions in the parameter space, known as shrimp-shapes [20,21]. As diagnostic tools we use the Lyapunov exponent to identify the shrimps. We also analyze the organization of these shrimp structures applying the concept of extreming curves [22].

This paper is organized as follow. Section 2 presents the Rulkov mapping and its dynamical properties. In Section 3 the parameter space is analyzed and the shrimp-shapes structures are characterized. Our final remarks are presented in Section 4.

2. The Rulkov mapping under a parametric perturbation

The model proposed by Rulkov is a two dimensional map in terms of the dynamical variables X_{n+1} and Y_{n+1} [18], and can be written as

$$R : \begin{cases} X_{n+1} &= \frac{\alpha}{1+X_n{}^2} + Y_n, \\ Y_{n+1} &= Y_n - \sigma\,(X_n - \rho)\,, \end{cases} \tag{1}$$

where X_n and Y_n are the fast and low scale variables, respectively, and α, ρ, and σ are the control parameters. We introduce a parametric perturbation in the Rulkov map, such as $\alpha \to \alpha(1 + b_n\epsilon)$, that leads the map to be written as

$$\tilde{R} : \begin{cases} X_{n+1} &= \frac{\alpha(1+b_n\epsilon)}{1+X_n{}^2} + Y_n, \\ Y_{n+1} &= Y_n - \sigma\,(X_n - \rho)\,, \end{cases} \tag{2}$$

where ϵ is a parametric perturbation, with $b_n = (-1)^n$ or $b_n = (-1)^{n+1}$. For $\epsilon = 0$ the traditional Rulkov map is recovered [11].

The successive application of the map given by Eq. (2) over an initial condition is shown in Fig. 1(a–d). Fig. 1(a) shows that the behavior of the fast variable X along the time is composed by the alternation of periodic and chaotic oscillations, known as bursts. The period of the bursts are linked with the oscillations of the low variable Y (see Fig. 1(b)). Every time the low variable reaches a characteristic maximum value, the period of bursts is initialized (green dashed lines). The opposite is also observed, so the end of bursts period happens when the low variable reaches a characteristic minimum value. Between chaotic bursts, one can see that there exist a period two behavior of the variable X. The control parameters have an interesting role in the dynamics of the problem, as shown in Fig. 1(c,d), the change of the control parameter α to 4.15 leads the dynamic to present bursts smoother than the observed in Fig. 1(a,b).

The phase space X vs Y from the Rulkov map is shown in Fig. 2, where the black curves represent the evolution of an initial condition starting from the blue arrow. An important aspects to understand the properties of the phase space is looking for the fixed points and how the initial condition are influence by them. For this, we made an approximation of the Eq. (2) for a one dimensional map

$$X_{n+1} = \frac{\alpha(1 + b_n\epsilon)}{1 + X_n{}^2} + \gamma_y, \tag{3}$$

where such approximation is possible because the low variable Y does not change too much in a small period of time, so allowing us to approach Y as a constant γ_y. It is important to remark that if we do $\epsilon = 0$ the traditional one dimensional Rulkov map found in the literature is recovered.

The fixed points X^* from the dynamics are found when the equation $X_{n+2} = f(X^*) = X^*$ is satisfied. If we start with $b_n = +1$, one can find the solution for

$$X_{n+2} = \frac{\alpha(1 + \epsilon)}{1 + \left[\frac{\alpha(1-\epsilon)}{1+(X^*)^2} + \gamma_y\right]^2} + \gamma_y = X^*. \tag{4}$$

This equation is not so simple to be solved analytically. But one can prove that this equation has five solutions $X^*_{j(+)}$, with $j = 1, 2, \ldots, 5$, that correspond to the fixed points of the dynamics. Similar procedure can be found when we start with

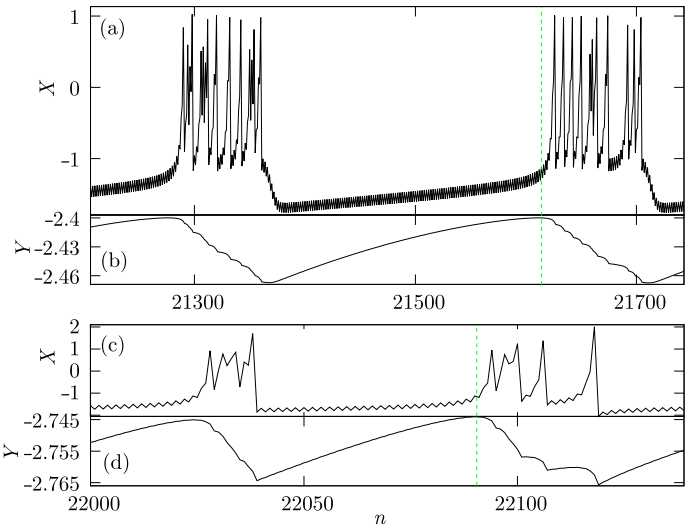

Fig. 1. (Color online) Time evolution of the variables: (a) X; (b) Y. The combination of control parameters are $\alpha = 3, \sigma = 0.001, \rho = -1.25$ and $\epsilon = 0.15$. The green dashed vertical line marks the beginning of the chaotic burst, which happens when the value of Y is maximum at item (b). In items (c,d) we have changed the value of α to 4.15.

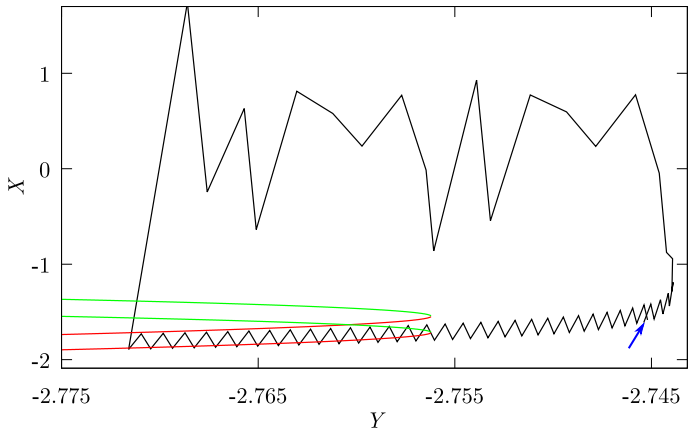

Fig. 2. Phase space X vs Y considering $\alpha = 4.15, \sigma = 0.001, \rho = -1.25$ and $\epsilon = 0.15$. The black curve is an orbit in the phase space, and we plotted only one cycle starting from the blue arrow. The red line represents the position of two stable period 2 fixed points obtained for the 1D version of the mapping, while the green curves represent two unstable period 2 fixed points.. (For interpretation of the references to color in this figure legend, the reader is referred to the web version of this article.)

$b_n = -1$, leading to the following equation

$$X_{n+2} = \frac{\alpha(1-\epsilon)}{1+\left[\frac{\alpha(1+\epsilon)}{1+(X^*)^2}+\gamma_y\right]^2} + \gamma_y = X^*, \tag{5}$$

which also has five solutions $X^*_{j(-)}$, with $j = 1, 2, \ldots, 5$. It is important to mention that some of the solutions are in the complex plane and some of them are real values.

We classify these fixed points studying the return map as presented in Fig. 3. The return map shows that initially the Rulkov map has three fixed points, been $X^*_{1(+)}$ and $X^*_{1(-)}$ stable, and $X^*_{2(+)}$, $X^*_{2(-)}$, $X^*_{3(+)}$ and $X^*_{3(-)}$ unstable (see Fig. 3(a)). However, when the parameter γ_y is increased, the fixed points $X^*_{1(+)}$, $X^*_{1(-)}$, $X^*_{2(+)}$ and $X^*_{2(-)}$ begin to approach each other until collide and disappear, as shown in Fig. 3(b,c). Only the fixed points $X^*_{3(+)}$ and $X^*_{3(-)}$ remains. In such a case, the other eight fixed points are in the complex plane.

A natural question that came from the analyze above is about the influence of the fixed point over the dynamics. To answer this question, we first plot the position of stable (unstable) fixed points over an orbit from the phase space of Fig. 2. As one can see, the orbit tends to follow the fixed points for a time interval until starting the chaotic burst.

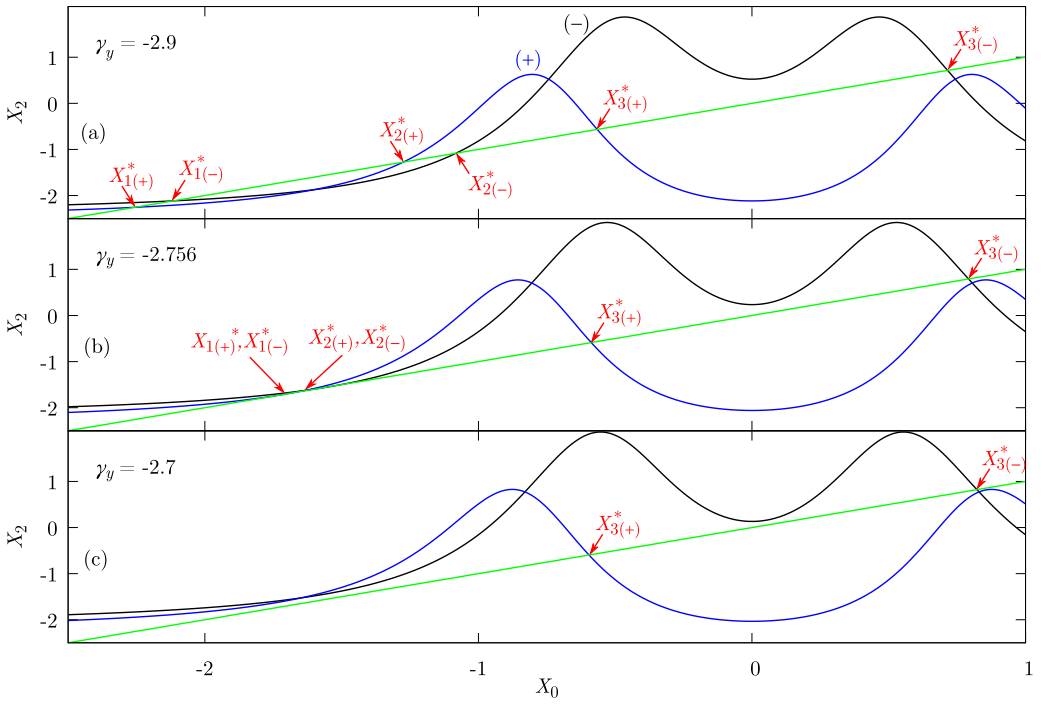

Fig. 3. (Color online) X_2 vs X_0 for different values of γ_y: (a) $\gamma_y = -2.9$; (b) $\gamma_y = -2.756$; (c) $\gamma_y = -2.7$. In (a) we have period two stable fixed points marked as $X^*_{1(+)}$ and $X^*_{1(-)}$ and four other period two fixed points are also observed, $X^*_{2(+)}$, $X^*_{2(-)}$, $X^*_{3(+)}$ and $X^*_{3(-)}$, but in this case they are unstable. In (b) $X^*_{1(+)}$ and $X^*_{1(-)}$ are approximately at the same position and the same for $X^*_{2(+)}$ and $X^*_{2(-)}$, indicating that a saddle–node bifurcation is observed. In item (c) only two period two fixed points, $X^*_{3(+)}$ and $X^*_{3(-)}$, remains. The other fixed points are in the complex plane, where we have a total of ten different solutions.

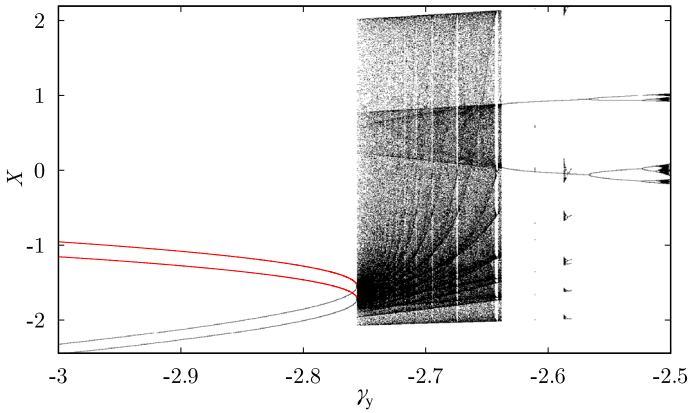

Fig. 4. Bifurcation diagram X vs γ_y for the one-dimensional version of the Rulkov map. In red we show two unstable period two fixed points.. (For interpretation of the references to color in this figure legend, the reader is referred to the web version of this article.)

If the bifurcation diagram is taken into account, as showing in Fig. 4, we see that the behavior of X changes from periodicity to chaotic oscillations (bursts) as γ_y is increased (decreased). It is interesting to note that a saddle–node bifurcation appears exactly when the fixed points $X^*_{1(+)}$, $X^*_{1(-)}$, $X^*_{2(+)}$ and $X^*_{2(-)}$ vanish from the dynamics and only after that, the bursts are initialized inside of the chaotic attractor. Therefore, when the attractor crises happens, the dynamics is forced to return to a stable behavior marking the end of the burst period.

3. Parameter space analysis

After the description above about the system dynamics, we find that depending on the control parameter an initial condition may exhibit chaotic or regular behaviors. However, when a small perturbation is added over the parameter, these behaviors can change. This information lead us to natural question about the parameter space, what happens with the system

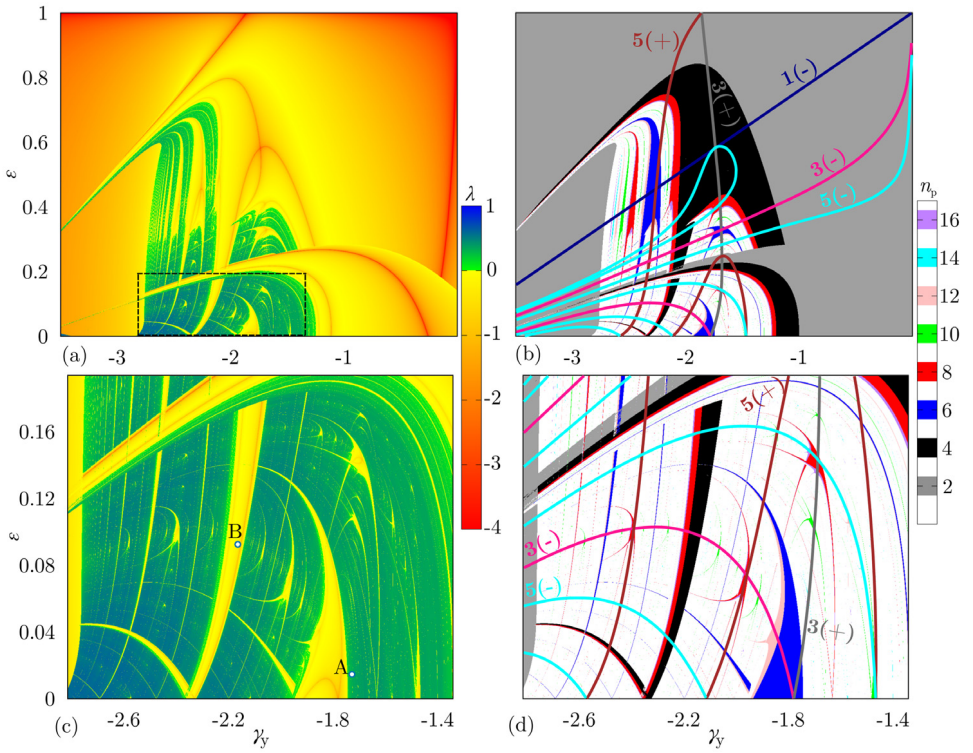

Fig. 5. Parameter space for ϵ vs γ_y. In items (a, c) we have considered as colors the Lyapunov exponents (λ), while in items (b, d) the colors represent the period of the shrimps, where lines are the extreming curves. The value of α chosen was 4.15.. (For interpretation of the references to color in this figure legend, the reader is referred to the web version of this article.)

if we simultaneously change the control parameters? To answer this question, we analyze the parameter space from the system using Lyapunov exponents to characterized regions where the control parameter leads the dynamic to chaos or regular motion.

For one dimensional system, the Lyapunov exponent [23] is given by

$$\lambda = \lim_{n\to\infty} \frac{1}{n} \sum_{i=1}^{n} \ln \left| \frac{\partial X_{n+1}}{\partial X_n} \right|, \tag{6}$$

where

$$\frac{\partial X_{n+1}}{\partial X_n} = -\frac{2\alpha X_n (1 + b_n \epsilon)}{\left(1 + {X_n}^2\right)^2}. \tag{7}$$

The classification of the exponent for one orbit shows that for $\lambda > 0$ a chaotic behavior is observed, while $\lambda < 0$ characterizes that the orbit is periodic or quasi-periodic. The parameter space ϵ vs γ_y for the Rulkov map are shown in Fig. 5(a, c).

In order to generate Figs. 5(a, c), we split in 1000 by 1000 different values of ϵ and γ_y. For each combination of parameters, we iterate mapping (3) up to 10^6 times. For the next 10^6 iterations the Lyapunov exponent λ (given by Eq. (6)) is computed. Figs. 5(a, c) present a set of colors, where red to yellow have negative values of λ, meaning that orbits are periodic in these regions, on the other hand, green to blue indicate regions of positive values of λ, meaning that the orbits tend to reach chaotic attractors. As one can see, there are many periodic self similar structures embedded in chaotic regions in the parameter space, such structures are known as shrimps-shapes. The characterization of the shrimps-shape can be done by the Lyapunov exponents as presented above, on the other hand, if we study the periodicity of the parameter space as made in Fig. 5(b, d), where the periods are indicated by colors, the self similar structures are still found. Observe that Fig. 5(c) is an enlargement of the black dashed rectangle in Fig. 5(a).

In order to find local maximums and minimums, one need to consider $\frac{\partial X_{n+1}}{\partial X_n} = 0$. As solution, we find $X^* = 0$, that is a local maximum. We consider $X_{n+1} = X_n = X^*$ to calculate the extreming curve with period 1, where it results in

$$\epsilon = -\frac{1}{b_n}\left(1 + \frac{\gamma_y}{\alpha}\right). \tag{8}$$

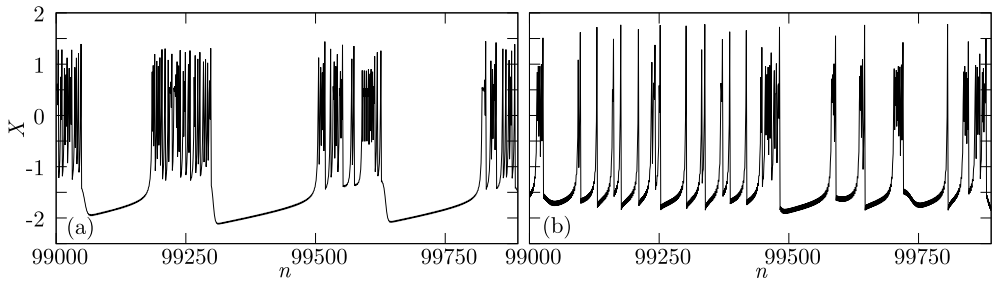

Fig. 6. (Color online) Time evolution of X for the two-dimensional version of our map. In (a) we show an orbit which starts in the chaotic region of Fig. 5(c) (marked as the point A in such a figure), while in (b) an orbit starting in the periodic region of Fig. 5(c) (marked as the point B in such a figure).

This curve is shown in Fig. 5(b) labeled as $1(-)$. The minus means that we start with $b_n = -1$ in Eq. (3), otherwise, the plus sign means that $b_n = +1$. The other extreming curves were found numerically, where the main idea to find these curves is as follows: if you want to find the period 3 extreming curve, choose 1000 by 1000 different values of γ_y and ϵ. For each combination of control parameters we start an orbit with initial condition given by $X_0 = X^*$ and $b_n = \pm 1$. After 3 iterations of the mapping (3) we check if the condition $|X_3 - X_0| < 10^{-3}$ is true. If it is true, it means that after 3 iterations the orbit returns to the initial condition $X_0 = X^*$. This orbit is not periodic because it only happens for even values of iterations. As an example, in Fig. 5(b), the curve $3(+)$ means that it is a period 3 extreming curve starting with $b_n = +1$. It is possible to obtain an infinity number of extreming curves, but we decided to show it until the period 5.

The extreming curves can be used to predict the position of the shrimps in the parameter space. The intercept between negative and positive extreming curves happens exactly in a periodic structure. For example, in Fig. 5(b) the intercept between curves $1(-)$ and $3(+)$ happens in the period 4 shrimp (extremings $1 + 3 = 4$). Another example is the intercept of $5(+)$ and $1(-)$, which happens in the period 6 shrimp ($5 + 1 = 6$). So, as conclusion, the position of the other shrimps can be found using the extreming curves, where some of them were highlighted in Figs. 5(b, d).

Now we compare the result obtained in Fig. 5(c) to the two-dimensional map (2), where we use $\alpha = 4.15$. If we take the coordinates of the point A in Fig. 5(c), given by $(\epsilon, \gamma_y) = (0.014596, -1.72767)$, one can start an orbit in the 2-D version of the mapping, considering $Y_n = \gamma_y$ and the other control parameters are set as $\sigma = 0.001$ and $\rho = -1.25$ (as used in Figs. 1 and 2). As result, in Fig. 6(a) we show the time evolution of an orbit which started in the chaotic region of Fig. 5(c). Now one can compare with an orbit that starts in a periodic region of Fig. 5(c). The point B, which is taken in $(\epsilon, \gamma_y) = (0.092508, -2.16444)$, is then used to produce Fig. 6(b). As one can see, if we use a chaotic region as shown in A, one can see that the burst size of the chaotic region is larger than the periodic region. As shown in Ref. [24], The periodicities of the burst follows a period-increasing pathway as known from the Arnol'd tongues, scaling in size with periodicity. As our system does not exhibit these Arnol'd tongues, it is very difficult to count the number spikes for each shrimp or periodic region taken in Fig. 5(c). More simulations are necessary in order to understand what is happening, but it is a first step trying to understand such a system, which does not exclude the results found here.

In a next work, one can explore this connection and try to reproduce results in systems with more than one neuronal membrane. We believe that this system will provide some interesting results when coupled systems are taken into account.

4. Conclusion

The Rulkov map is phenomenological model that simulates the changes in the neuronal membrane potential. In this work, we introduced a parametric perturbation in this system, where it can be related to a malfunction of a neuronal membrane. It was shown that the system still keeps its main characteristics, presenting periodic behavior, followed by chaotic bursts. We found the fixed points exhibited by the system and analyzed their stability through the return maps. We showed that the chaotic oscillations of the dynamics were initialized when a saddle–node bifurcation happened, however, when the attractor crisis was observed, the chaotic motion was forced to return to a regular regime. In the final part of this paper, we characterized chaotic and regular regions in the parameter space. Such study revealed some periodic self similar structures, known as shrimp-shapes, that emerged from chaotic regions. Through the concept of returning curves, the organization of these structures were described.

Acknowledgments

DRC acknowledges PNPd/CAPES. MH thanks to CAPES, Brazil for the financial support and AMB thanks CNPq, Brazil.

References

[1] J.A. de Oliveira, E.R. Papesso, E.D. Leonel, Relaxation to fixed points in the logistic and cubic maps: Analytical and numerical investigation, Entropy 15 (2013) 4310–4318.
[2] P.M. Gade, G.G. Sahasrabudhe, Universal persistence exponent in transition to antiferromagnetic order in coupled logistic maps, Phys. Rev. E 87 (2013) 052905.
[3] K. Hamacher, Dynamical regimes due to technological change in a microeconomical model of production, Chaos 22 (2012) 033149.
[4] R.M. May, G.A. Oster, Bifurcation and dynamical systems in simple ecological models, Am. Nat. 110 (1976) 573–599.
[5] E.L. Lameu, S.F. Borges, R.R. Borges, K.C. Iarosz, I. Caldas, A.M. Batista, R.L. Viana, J. Kurths, Suppression of phase synchronisation in network based on cat's brain, Chaos 26 (2016) 043107.
[6] T.Y. Li, J.A. Yorke, Period three implies chaos, Appl. Math. Model. 82 (1975) 985–992.
[7] M.J. Feigenbaum, Quantitative universality for a class of non-linear transformations, J. Stat. Phys. 19 (1978) 25–52.
[8] Y. Pomeau, P. Manneville, Intermittent transition to turbulence in dissipative dynamical systems, Commun. Math. Phys. 74 (1980) 189–197.
[9] D. Ilhem, K. Amel, One-dimensional and two-dimensional dynamics of cubic maps, Discrete Dyn. Nat. Soc. 2006 (2006) 15840.
[10] M. Hansen, D.R. Costa, D.F.M. Oliveira, E.D. Leonel, Statistical properties for a dissipative model of relativistic particles in a wave packet: A parameter space investigation, Appl. Math. Comput. 238 (2014) 387–392.
[11] N.F. Rulkov, Modeling of spiking–bursting neural behavior using two-dimensional map, Phys. Rev. E 65 (2002) 041922.
[12] E.L. Lameu, F.S. Borges, R.R. Borges, A.M. Batista, M.S. Baptista, R.L. Viana, Network induces burst synchronisation in cat cerebral cortex, Commun. Nonlinear Sci. Numer. Simul. 34 (2016) 45–54.
[13] L. Fronzoni, M. Giocondo, M. Pettini, Experimental evidence of suppression of chaos by resonant parametric perturbations, Phys. Rev. A 43 (1991) 6483–6487.
[14] R. Meucci, W. Gadomski, M. Ciofini, F.T. Arecchi, Experimental control of chaos by means of weak parametric perturbations, Phys. Rev. E 94 (1994) 2528–2531.
[15] K.A. Mirus, J.C. Sprott, Controlling chaos in a high dimensional system with periodic parametric perturbations, Phys. Lett. A 254 (1999) 275–278.
[16] V.V. Astakhov, V.S. Anishchenko, T. Kapitaniak, A.V. Shabunin, Synchronization of chaotic oscillators by periodic parametric perturbations, Physica D 109 (1997) 11–16.
[17] P. Deivasundari, R. Geetha, G. Uma, Murali K. Chaos, bifurcation and intermittent phenoena in DC-DC converters under resonant parametric perturbation, Eur. Phys. J. Spec. Top. 222 (2013) 689–697.
[18] N.F. Rulkov, Regularization of synchronized chaotic bursts, Phys. Rev. Lett. 86 (2001) 183–186.
[19] N. Ozkucur, K.P. Quinn, J. Pang, C. Du, I. Georgakoudi, E.L. Miller, M. Levin, D.L. Kaplan, Membrane potential depolarization causes alterations in neuron arrangement and connectivity in cocultures, Brain Behav 5 (2015) 24–38.
[20] J.A.C. Gallas, Structure of the parameter space of the Hénon map, Phys. Rev. Lett. 70 (1983) 2714.
[21] E.S. Medeiros, S.L.T. de Souza, T.R.O. Medrano, I.L. Caldas, Replicate periodic windows in the parameter space of driven oscillators, Chaos Solitons Fractals 44 (2011) 982.
[22] D.R. da Costa, M. Hansen, G. Guarise, T.R.O. Medrano, E.D. Leonel, The role of extreme orbits in the global organization of periodic regions in parameter space for one dimensional maps, Phys. Lett. A 380 (2016) 1610.
[23] T. Alligood, T.D. Sauer, J.A. Yorke, Chaos: An Introduction To Dynamical Systems, Springer-Verlag, New York, 1996.
[24] F. Gomez, R.L. Stoop, R. Stoop, Universal dynamical properties preclude standard clustering in a large class of biochemical data, Bioinformatics 30 (2014) 2486–2493.